

## Low-Pressure Electrochemical Synthesis of Complex High-Pressure Superconducting Superhydrides

Pin-Wen Guan<sup>1</sup>, Ying Sun,<sup>2</sup> Russell J. Hemley,<sup>3</sup> Hanyu Liu<sup>1</sup>,<sup>2</sup>  
Yanming Ma<sup>2,4</sup> and Venkatasubramanian Viswanathan<sup>1,5,\*</sup>

<sup>1</sup>Department of Mechanical Engineering, Carnegie Mellon University, Pittsburgh, Pennsylvania 15213, USA

<sup>2</sup>International Center of Computational Method and Software and State Key Laboratory for Superhard Materials, College of Physics, Jilin University, Changchun 130012, China

<sup>3</sup>Departments of Physics, Chemistry, and Earth and Environmental Sciences, University of Illinois Chicago, Chicago, Illinois 60607, USA

<sup>4</sup>International Center of Future Science, Jilin University, Changchun 130012, China

<sup>5</sup>Department of Physics, Carnegie Mellon University, Pittsburgh, Pennsylvania 15213, USA



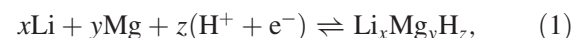
(Received 7 October 2021; accepted 15 March 2022; published 6 May 2022)

There is great current interest in multicomponent superhydrides due to their unique quantum properties under pressure. A remarkable example is the ternary superhydride  $\text{Li}_2\text{MgH}_{16}$  computationally identified to have an unprecedented high superconducting critical temperature  $T_c$  of  $\sim 470$  K at 250 GPa. However, the very high synthesis pressures required remains a significant hurdle for detailed study and potential applications. In this Letter, we evaluate the feasibility of synthesizing ternary Li-Mg superhydrides by the recently proposed pressure-potential ( $\mathcal{P}^2$ ) method that uniquely combines electrochemistry and applied pressure to control synthesis and stability. The results indicate that it is possible to synthesize Li-Mg superhydrides at modest pressures by applying suitable electrode potentials. Using pressure alone, no Li-Mg ternary hydrides are predicted to be thermodynamically stable, but in the presence of electrode potentials, both  $\text{Li}_2\text{MgH}_{16}$  and  $\text{Li}_4\text{MgH}_{24}$  can be stabilized at modest pressures. Three polymorphs are predicted as ground states of  $\text{Li}_2\text{MgH}_{16}$  below 300 GPa, with transitions at 33 and 160 GPa. The highest pressure phase is superconducting, while the two at lower pressures are not. Our findings point out the potentially important role of the  $\mathcal{P}^2$  method in controlling phase stability of complex multicomponent superhydrides.

DOI: 10.1103/PhysRevLett.128.186001

There has been enormous recent progress in the quest for room-temperature superconductors, enabled by superhydrides containing large amounts of hydrogen. The first near-room-temperature superconductor was predicted [1,2], synthesized [3], discovered [4], and subsequently confirmed [5] in the La-H system. Recently, a room-temperature superconductor was discovered in the C-S-H system [6]. In addition, the same theoretical techniques that led to the discovery of superconductivity in  $\text{LaH}_{10}$  predict even higher-temperature superconductors such as  $\text{Li}_2\text{MgH}_{16}$  with  $T_c$  as high as  $\sim 470$  K at 250 GPa [7]. However, creation of these superhydrides requires megabar ( $> 100$  GPa) pressure, which is a significant hurdle for large-scale synthesis. Therefore, lowering the pressure for synthesizing these novel materials is a crucial milestone in the pursuit of practical room-temperature superconductivity [8]. Here, we show that a recently proposed novel strategy for synthesizing superhydrides in which electrochemistry and pressure are combined can be used to stabilize high pressure multicomponent hydrides. Focusing on the ternary Li-Mg-H system, we demonstrate the possible synthesis of Li-Mg superhydrides at modest pressures.

Our pressure-potential ( $\mathcal{P}^2$ ) strategy combines electrochemistry and pressure to control the phase stability with more degrees of freedom than either of those control variables alone [9]. We consider the following loading reaction as an example:



with the associated Gibbs energy change of the reaction

$$\Delta G = G_{\text{Li}_x\text{Mg}_y\text{H}_z} - xG_{\text{Li}} - yG_{\text{Mg}} - zG_{\text{H}^+} - zG_{\text{e}^-}. \quad (2)$$

The above equation can be further expressed as

$$\begin{aligned} \Delta G = & G_{\text{Li}_x\text{Mg}_y\text{H}_z} - xG_{\text{Li}} - yG_{\text{Mg}} \\ & - zG_{\text{H(stable)}} + zeU_{\text{SHE}} - zk_B T \ln(a_{\text{H}^+}), \end{aligned} \quad (3)$$

where  $a_{\text{H}^+}$  is the proton activity,  $U_{\text{SHE}}$  is the electrode potential referenced to the standard hydrogen electrode (SHE) generalized to high pressure regimes, and  $\text{H(stable)}$

denotes the stable phase of hydrogen which may be fluid or solid depending on the pressure.

Equation (3) shows that the phase stability of a Li-Mg hydride can be controlled by Li:Mg ratio, electrode potential, pH, and pressure as it affects Gibbs energies of the involved phases. To make the calculated electrochemical phase diagram more compact, the reversible hydrogen electrode (RHE) can be used as the reference instead of the SHE to eliminate the explicit pH dependence

$$\Delta G = G_{\text{Li}_x\text{Mg}_y\text{H}_z} - xG_{\text{Li}} - yG_{\text{Mg}} - zG_{\text{H(stable)}} + zeU_{\text{RHE}}. \quad (4)$$

where  $U_{\text{RHE}}$  is the electrode potential referenced to the RHE and satisfies  $U_{\text{RHE}} = U_{\text{SHE}} - (k_B T/e) \ln(a_{\text{H}^+})$ . Negative electrode potentials, ( $U_{\text{RHE}} < 0$ ), provide driving force for increasing hydrogenation but, also, promote the competing hydrogen evolution reaction (HER), which may be kinetically suppressed by superconcentrated electrolytes or other mechanisms [10].

We examined the electrochemical phase stability of the Li-Mg-H system under pressure using density functional theory [11,12] calculations by the BEEF-vdW exchange correlation functional [13]. The calculations were run using the GPAW code [14,15] in the Atomic Simulation Environment [16]. Only stoichiometric phases were considered, with a total of 36 compositions, besides the pure substances, including nine binaries and 27 ternaries. The crystal structures were identified by the particle swarm optimization [17] using the CALYPSO code [18], with part of them already obtained in a previous Letter [7] and additional structures reported here. Additional details can be found in the Supplemental Material [19].

Theoretically calculated pressure dependent electrochemical Pourbaix diagrams for Li-Mg-H at 300 K are shown in Fig. 1. It is found that the phase equilibria depend on the Li:Mg ratio. At zero potential ( $U_{\text{RHE}} = 0$ ), for any Li:Mg ratio, no ternary Li-Mg hydrides are thermodynamically stable within the range of conditions studied, consistent with previous work [7]. The phase equilibrium is dominated by  $\text{MgH}_2 + \text{LiH}$  from ambient pressures to  $\sim 100$  GPa, above which a transition sequence  $\text{MgH}_4 + \text{LiH} \rightarrow \text{MgH}_4 + \text{LiH}_2 \rightarrow \text{MgH}_4 + \text{LiH}_8 \rightarrow \text{MgH}_4 + \text{LiH}_6 \rightarrow \text{MgH}_{16} + \text{LiH}_6 \rightarrow \text{MgH}_{12} + \text{LiH}_6$  occurs. Applying positive potential ( $U_{\text{RHE}} > 0$ ), Mg or Li metals,  $\text{Mg} + \text{LiH}$  and  $\text{MgH}_2 + \text{LiH}_2$  are stabilized. Interestingly, applying a negative potential ( $U_{\text{RHE}} < 0$ ), ternary Li-Mg superhydrides are stabilized at ambient and modest pressures. For a Li:Mg ratio 0–0.25,  $\text{LiH} + \text{Li}_2\text{MgH}_{16}$ ,  $\text{LiH} + \text{Li}_4\text{MgH}_{24}$ , and  $\text{LiH}_8 + \text{Li}_4\text{MgH}_{24}$  can be accessed with gradually lowered potential. For a Li:Mg ratio 0.25–0.5, the accessible phase equilibria become  $\text{LiH} + \text{Li}_2\text{MgH}_{16}$ ,  $\text{Li}_2\text{MgH}_{16} + \text{Li}_4\text{MgH}_{24}$ , and  $\text{MgH}_{16} + \text{Li}_4\text{MgH}_{24}$ . For a Li:Mg ratio above 0.5, the accessible

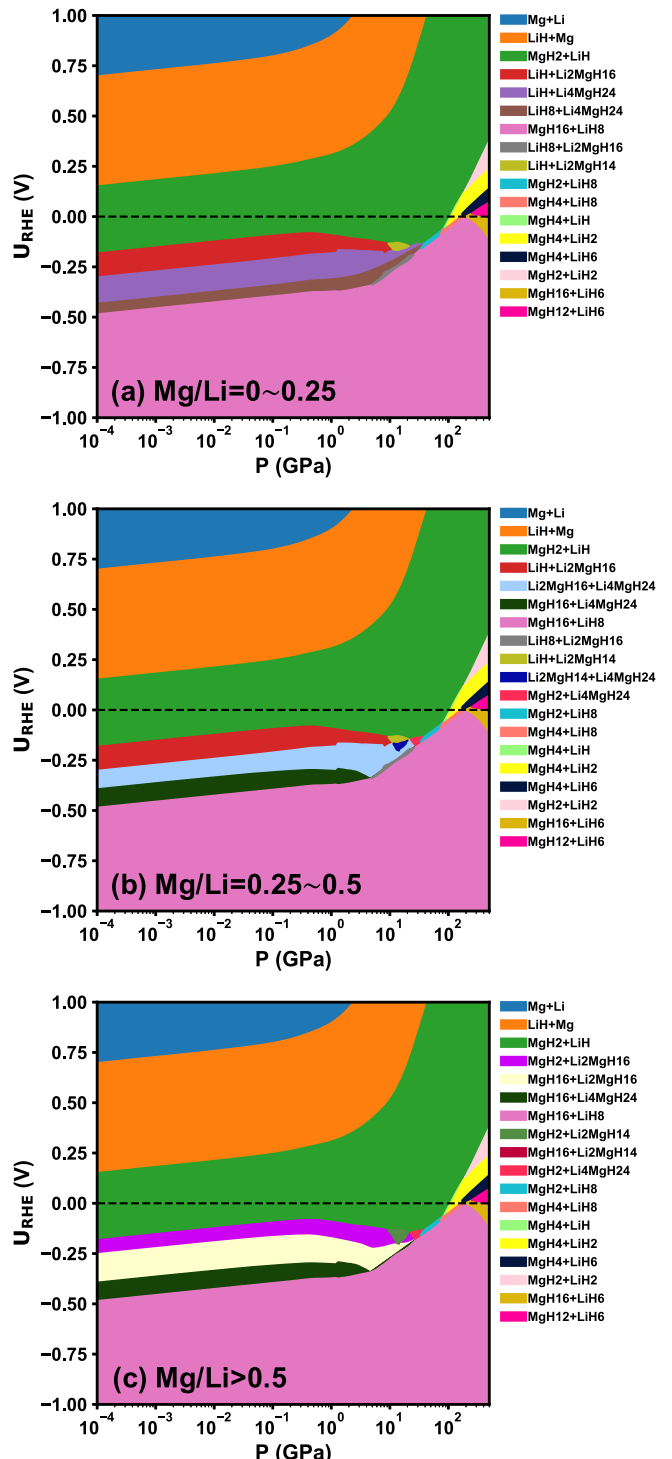


FIG. 1. Pressure dependent Pourbaix diagram of Li-Mg-H at 300 K by the best-fit BEEF-vdW functional [13]. The dashed line represents the equilibrium HER (hydrogen evolution reaction). Different phase regions are represented by different colors. Generally, each phase region has two phases coexisting. The potential in the diagrams is referenced to RHE and is actually pH-dependent if converted to the SHE scale.

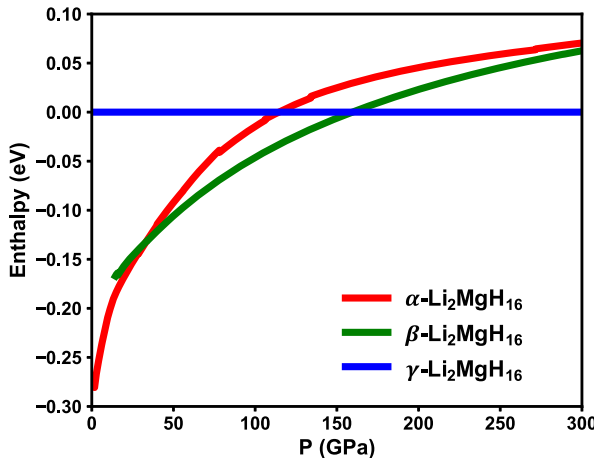


FIG. 2. Pressure dependent enthalpies of the three ground states of  $\text{Li}_2\text{MgH}_{16}$ .

phase equilibria are predicted to be  $\text{MgH}_2 + \text{Li}_2\text{MgH}_{16}$ ,  $\text{MgH}_{16} + \text{Li}_2\text{MgH}_{16}$ , and  $\text{MgH}_{16} + \text{Li}_4\text{MgH}_{24}$ . It can be seen that, among the multiple ternary compositions considered,  $\text{Li}_2\text{MgH}_{16}$  and  $\text{Li}_4\text{MgH}_{24}$  are the only two that are thermodynamically favorable at modest conditions, and their stability regions can be maximized under Mg-rich and Li-rich conditions, respectively.

We note that, near ambient pressure, the  $U$ - $\log P$  phase boundaries are nearly linear, with an order of magnitude reduction of the transition pressure achievable by only 0.03 V change in the electrode potential, as observed previously for binary hydride systems [9]. This is due to the dominant effect of pressure on the Gibbs energy of hydrogen gas, with the pressure-dependent part as  $\frac{1}{2}k_B T \ln(P)$  (using the ideal gas approximation) in the low pressure regime [9]. The regimes beyond low pressure have more complex pressure-dependent Gibbs energies for fluid and solid phases and the phase boundaries become much more sophisticated.

The ground state (the lowest enthalpy polymorph) at the corresponding pressure is considered for each composition in Fig. 1. Thus, even with the same stoichiometry, the

crystal structure may change at varying pressures, which is exemplified for  $\text{Li}_2\text{MgH}_{16}$  in Fig. 2. Based on the calculated enthalpies of the structures examined, it is found that  $\text{Li}_2\text{MgH}_{16}$  composition can form three polymorphs up to 300 GPa, which are termed as the  $\alpha$ ,  $\beta$ , and  $\gamma$  phases.  $\text{Li}_2\text{MgH}_{16}$  undergoes two polymorphic transitions,  $\alpha \rightarrow \beta$  at 33 GPa and  $\beta \rightarrow \gamma$  at 160 GPa. In addition, only  $\alpha\text{-Li}_2\text{MgH}_{16}$  can be thermodynamically stabilized provided HER is suppressed, while  $\beta\text{-Li}_2\text{MgH}_{16}$  and  $\gamma\text{-Li}_2\text{MgH}_{16}$  are both unfavorable (Fig. 1). However, it may still be possible to synthesize them, as the decomposition into hydrides with different stoichiometries is a diffusional phase transformation and kinetically controlled [22]. The  $Fd\bar{3}m$  phase with  $T_c$  reaching  $\sim 470$  K at 250 GPa [7] and a broad range of  $T_c$ 's estimated in more recent calculations that include anharmonicity and nuclear quantum effects [23] is found to be metastable with respect to the ground-state polymorphs within the conditions studied, in agreement with the previous Letter [7]. Interestingly, the coexistence of significant proton quantum diffusion together with hydrogen-induced superconductivity has been recently found in the  $Fd\bar{3}m$  phase [23], reminiscent of the prediction of superconducting superfluid hydrogen [24].

The crystal structures of the three polymorphs of  $\text{Li}_2\text{MgH}_{16}$  are shown in Fig. 3. Both  $\alpha\text{-Li}_2\text{MgH}_{16}$  and  $\beta\text{-Li}_2\text{MgH}_{16}$  have low symmetry with the  $P1$  space group.  $\alpha\text{-Li}_2\text{MgH}_{16}$  can be described as periodic corrugated hydrogenated Li-Mg layers filled with hydrogen dimers in between.  $\beta\text{-Li}_2\text{MgH}_{16}$  also has hydrogenated Li-Mg layers, but they are connected by sharing part of the coordinating hydrogen atoms. Compared with the two phases at lower pressure regimes,  $\gamma\text{-Li}_2\text{MgH}_{16}$  has higher symmetry with the  $P\bar{3}m1$  space group. It has a 3D network consisting of face-sharing Li-Mg-centered H-cage structures. Figure 4 details the effect of pressure on the H-H separation and the excess charge based on Bader's theory [25] for the  $\text{H}_2$  dimers found in  $\text{Li}_2\text{MgH}_{16}$ . It can be seen that a larger H-H separation usually correlates with a higher excess charge, consistent with the previous Letter [7]. The polymorphic transitions produce dramatic effects on H-H

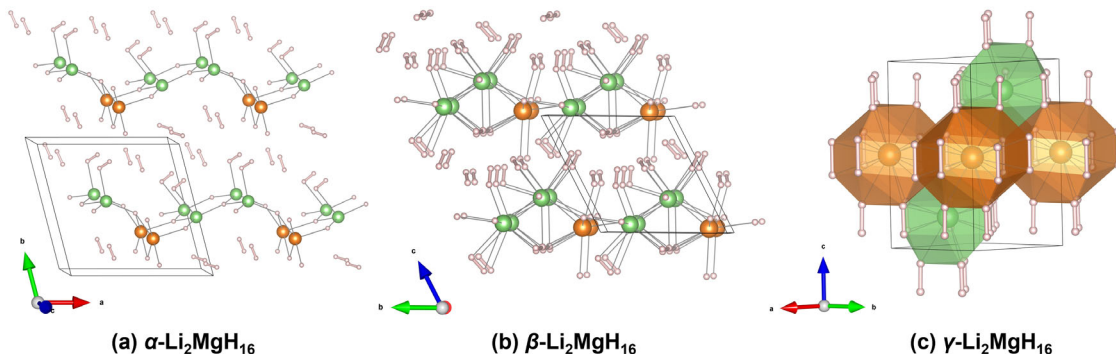


FIG. 3. Crystal structures of the three ground states of  $\text{Li}_2\text{MgH}_{16}$  at different pressures: (a)  $\alpha\text{-Li}_2\text{MgH}_{16}$  at 0–33 GPa, (b)  $\beta\text{-Li}_2\text{MgH}_{16}$  at 33–160 GPa, and (c)  $\gamma\text{-Li}_2\text{MgH}_{16}$  at  $> 160$  GPa.

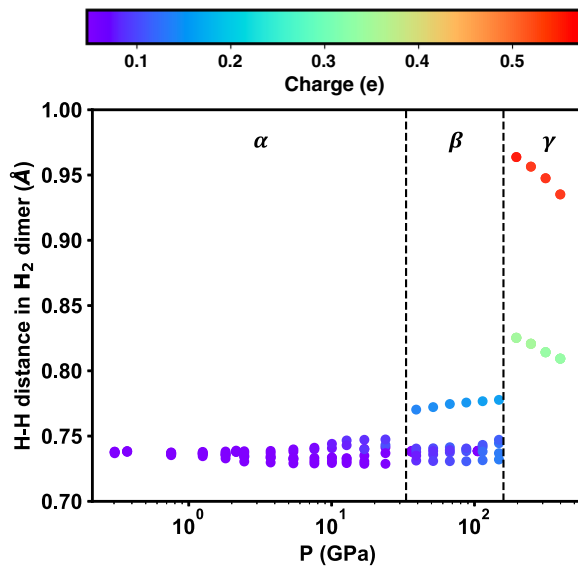


FIG. 4. Pressure dependent H-H separation in H<sub>2</sub> dimers and excess charge per H<sub>2</sub> dimer of Li<sub>2</sub>MgH<sub>16</sub> by the best-fit BEEF-vdW functional [13].

distances.  $\alpha$ -Li<sub>2</sub>MgH<sub>16</sub> and  $\beta$ -Li<sub>2</sub>MgH<sub>16</sub> have H-H separations smaller than 0.8 Å and an excess charge lower than 0.2e, while the maximum H-H distance and the excess charge in  $\gamma$ -Li<sub>2</sub>MgH<sub>16</sub> achieve 0.97 Å and 0.57e, respectively, within the pressure range studied. The increasing charge transfer from Li-Mg to H with pressure can be attributed to the increasing electronegativity difference between Li-Mg and H with pressure [26].

The electronic density of states (DOS) of  $\alpha$ -Li<sub>2</sub>MgH<sub>16</sub> and  $\beta$ -Li<sub>2</sub>MgH<sub>16</sub> are shown in Figs. 5(a) and 5(b), respectively. For these two phases, an energy gap separates the filled valence band and the unfilled conduction band, with zero DOS at the Fermi level, indicating that they are not conducting. The superconducting critical temperature  $T_c$  of  $\gamma$ -Li<sub>2</sub>MgH<sub>16</sub> based on the Eliashberg equation [27] is shown in Fig. 5(c), with Coulomb pseudopotential parameters of  $\mu^* = 0.10$  and  $\mu^* = 0.13$  adopted. The predicted  $T_c$  of  $\gamma$ -Li<sub>2</sub>MgH<sub>16</sub> increases with decreasing pressure from 250 to 150 GPa, reaching 177–193 K at 150 GPa. This trend is similar with that of the  $Fd\bar{3}m$  phase with decreasing pressure from 500 to 250 GPa [7]. The large difference in superconductivity between  $\alpha$  or  $\beta$ -Li<sub>2</sub>MgH<sub>16</sub> and  $\gamma$ -Li<sub>2</sub>MgH<sub>16</sub> is correlated with the presence of H<sub>2</sub> units in the former [7]. These results show that the most stable polymorphs of Li-Mg superhydrides at modest pressures are not superconducting, which may be overcome by optimizing the metal elements used. For example, computational studies of the La-B-H system predict that the composition LaBH<sub>8</sub> exhibits a  $T_c$  of 126–155 K at a relatively low pressure of ~50 GPa, although it is not thermodynamically stable against the ternary La-B-H hull below 110 GPa [28,29]. Thus, it is possible to design alloy composition of superhydrides having superconducting

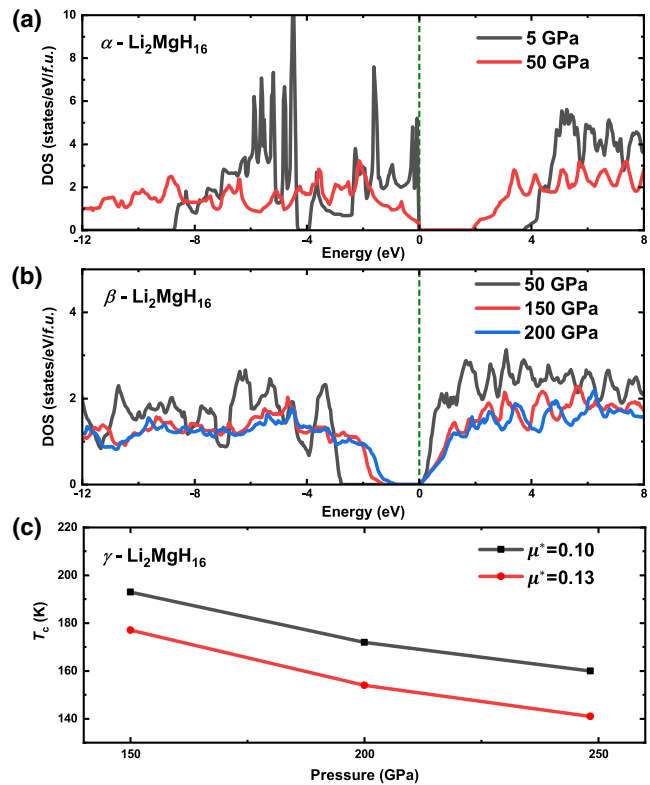


FIG. 5. (a) Electronic density of states of  $\alpha$ -Li<sub>2</sub>MgH<sub>16</sub>, (b) density of states of  $\beta$ -Li<sub>2</sub>MgH<sub>16</sub>, and (c) superconducting critical temperature of  $\gamma$ -Li<sub>2</sub>MgH<sub>16</sub>.

ground-state polymorphs at modest pressures. In addition, metastable polymorphs can be kinetically favored, such as the Pd<sub>3</sub>H<sub>4</sub> phase with a Cu<sub>3</sub>Au-type ordering of the Pd or vacancy lattice [9,30].

In conclusion, this Letter predicts the possibility of synthesizing ternary Li-Mg superhydrides at modest pressures by the  $\mathcal{P}^2$  method. For hydride systems, high  $T_c$  superconductivity correlates with highly H-rich compositions and characterized structural features. The  $\mathcal{P}^2$  method can effectively enhance stability of highly H-rich compositions at modest conditions; further realizing structural features for superconductivity within a given stoichiometry still remains an open question, but may be achieved by synthesis of kinetically stabilized phases given that the present analysis is based on thermodynamic stability. Such a synthesis pathway could be addressed by experimental and further theoretical efforts. Design of suitable types of metals in hydrides is also an important aspect, which can be accelerated by machine learning techniques. In practice, the highest achievable hydrogenation will depend on suppressing HER and on engineering issues like maintaining structural integrity of the highly hydrogenated electrode, which may be tackled by microstructure design. The value of the  $\mathcal{P}^2$  method is creating new space for controlling phase stability and for synthesizing materials with new stoichiometries or materials with existing stoichiometries

but novel structures. The power to unlock new phases can be further amplified when coupled with increasing the number of chemical constituents, as evident by the important ternary Li-Mg-H system studied here.

This work was supported by Google, the U.S. National Science Foundation (DMR-2104881) and the Department of Energy-National Nuclear Security Administration (DE-NA0003975). Y. S., H. L., and Y. M. would like to acknowledge funding support from the Natural Science Foundation of China under Grant No. 52090024. The authors would like to thank Yet-Ming Chiang, Matt Trevithick, Karen Sugano, and Florian Metzler for helpful discussions.

V. V. and P. G. are inventors on a provisional patent application, No. 63/028,265, related to electrochemical synthesis of superhydrides.

\*venkvis@cmu.edu

- [1] H. Liu, I. I. Naumov, R. Hoffmann, N. W. Ashcroft, and R. J. Hemley, *Proc. Natl. Acad. Sci. U.S.A.* **114**, 6990 (2017).
- [2] F. Peng, Y. Sun, C. J. Pickard, R. J. Needs, Q. Wu, and Y. Ma, *Phys. Rev. Lett.* **119**, 107001 (2017).
- [3] Z. M. Geballe, H. Liu, A. K. Mishra, M. Ahart, M. Somayazulu, Y. Meng, M. Baldini, and R. J. Hemley, *Angew. Chem., Int. Ed. Engl.* **57**, 688 (2018).
- [4] M. Somayazulu, M. Ahart, A. K. Mishra, Z. M. Geballe, M. Baldini, Y. Meng, V. V. Struzhkin, and R. J. Hemley, *Phys. Rev. Lett.* **122**, 027001 (2019).
- [5] A. P. Drozdov, P. P. Kong, V. S. Minkov, S. P. Besedin, M. A. Kuzovnikov, S. Mozaffari, L. Balicas, F. F. Balakirev, D. E. Graf, V. B. Prakapenka, E. Greenberg, D. A. Knyazev, M. Tkacz, and M. I. Eremets, *Nature (London)* **569**, 528 (2019).
- [6] E. Snider, N. Dasenbrock-Gammon, R. McBride, M. Debessai, H. Vindana, K. Vencatasamy, K. V. Lawler, A. Salamat, and R. P. Dias, *Nature (London)* **586**, 373 (2020).
- [7] Y. Sun, J. Lv, Y. Xie, H. Liu, and Y. Ma, *Phys. Rev. Lett.* **123**, 097001 (2019).
- [8] J. Lv, Y. Sun, H. Liu, and Y. Ma, *Matter Radiat. Extremes* **5**, 068101 (2020).
- [9] P.-W. Guan, R. J. Hemley, and V. Viswanathan, *Proc. Natl. Acad. Sci. U.S.A.* **118**, e2110470118 (2021).
- [10] L. Suo, O. Borodin, T. Gao, M. Olguin, J. Ho, X. Fan, C. Luo, C. Wang, and K. Xu, *Science* **350**, 938 (2015).
- [11] P. Hohenberg and W. Kohn, *Phys. Rev.* **136**, B864 (1964).
- [12] W. Kohn and L. J. Sham, *Phys. Rev.* **140**, A1133 (1965).
- [13] J. Wellendorff, K. T. Lundgaard, A. Møgelhøj, V. Petzold, D. D. Landis, J. K. Nørskov, T. Bligaard, and K. W. Jacobsen, *Phys. Rev. B* **85**, 235149 (2012).
- [14] J. J. Mortensen, L. B. Hansen, and K. W. Jacobsen, *Phys. Rev. B* **71**, 035109 (2005).
- [15] J. Enkovaara *et al.*, *J. Phys. Condens. Matter* **22**, 253202 (2010).
- [16] A. H. Larsen *et al.*, *J. Phys. Condens. Matter* **29**, 273002 (2017).
- [17] Y. Wang, J. Lv, L. Zhu, and Y. Ma, *Phys. Rev. B* **82**, 094116 (2010).
- [18] Y. Wang, J. Lv, L. Zhu, and Y. Ma, *Comput. Phys. Commun.* **183**, 2063 (2012).
- [19] See Supplemental Material at <http://link.aps.org/supplemental/10.1103/PhysRevLett.128.186001> for calculations of Gibbs energies, which includes Refs. [20,21].
- [20] P. Vinet, J. R. Smith, J. Ferrante, and J. H. Rose, *Phys. Rev. B* **35**, 1945 (1987).
- [21] *NIST Chemistry WebBook, NIST Standard Reference Database Number 69*, edited by P. Linstrom and W. Mallard (National Institute of Standards and Technology, Gaithersburg, 2022).
- [22] R. W. Balluffi, S. M. Allen, and W. C. Carter, *Kinetics of Materials* (John Wiley & Sons, New York, 2005).
- [23] H. Wang, Y. Yao, F. Peng, H. Liu, and R. J. Hemley, *Phys. Rev. Lett.* **126**, 117002 (2021).
- [24] E. Babaev, A. Sudbø, and N. W. Ashcroft, *Nature (London)* **431**, 666 (2004).
- [25] R. F. Bader, *Acc. Chem. Res.* **18**, 9 (1985).
- [26] M. Rahm, R. Cammi, N. W. Ashcroft, and R. Hoffmann, *J. Am. Chem. Soc.* **141**, 10253 (2019).
- [27] G. Eliashberg, *Sov. Phys. JETP-USSR* **11**, 696 (1960).
- [28] S. Di Cataldo, C. Heil, W. von der Linden, and L. Boeri, *Phys. Rev. B* **104**, L020511 (2021).
- [29] X. Liang, A. Bergara, X. Wei, X. Song, L. Wang, R. Sun, H. Liu, R. J. Hemley, L. Wang, G. Gao, and Y. Tian, *Phys. Rev. B* **104**, 134501 (2021).
- [30] Y. Fukai and N. Ōkuma, *Phys. Rev. Lett.* **73**, 1640 (1994).